Article:
Montanari, E, Oates, A orcid.org/0000-0003-0519-4556, Di Meo, C et al. (8 more authors) (2018) Hyaluronan-Based Nanohydrogels for Targeting Intracellular S. Aureus in Human Keratinocytes. Advanced Healthcare Materials, 7 (12). 1701483. ISSN 2192-2640

https://doi.org/10.1002/adhm.201701483

Full paper

Hyaluronan-Based Nanohydrogels for Targeting Intracellular *S. aureus* in Human Keratinocytes

Elita Montanari, Angela Oates, Chiara Di Meo, Josephine Meade, Rugiada Cerrone, Antonio Francioso, Deirdre Devine, Tommasina Coviello, Patrizia Mancini, Luciana Mosca* and Pietro Matricardi*

Dr. E. Montanari, Dr. C. Di Meo, R. Cerrone, Prof. T. Coviello, Dr. P. Matricardi, Department of Drug Chemistry and Technologies, Sapienza University of Rome, P.le Aldo Moro 5, 00185, Rome, IT

Dr. A. Oates, School of Healthcare, Faculty of Medicine and Health, University of Leeds, LS2 9JT, Leeds, UK

Dr. J. Meade, Division of Oral Biology, School of Dentistry, University of Leeds, LS7 9TF, Leeds, UK

Prof. D. Devine, Division of Oral Biology, School of Dentistry, Faculty of Medicine and Health, University of Leeds, LS2 9LU, Leeds, UK

Dr. A. Francioso, Dr. L. Mosca, Department of Biochemical Sciences "A. Rossi Fanelli", Sapienza University of Rome, P.le Aldo Moro 5, 00185, Rome, IT

Prof. P. Mancini, Department of Experimental Medicine, Sapienza University of Rome, V.le Regina Elena 291, 00161, Rome, IT.

E-mail: pietro.matricardi@uniroma1.it

E-mail: luciana.mosca@uniroma1.it

Keywords: Intracellular infections, hyaluronan, nanohydrogels, keratinocytes, antibiotic delivery

Abstract

Staphylococcus aureus is one of the most significant human pathogens that is frequently isolated in a wide range of superficial and systemic infections. The ability of *S. aureus* to invade and survive within host cells such as keratinocytes and host immune cells has been increasingly recognised as a potential factor in persistent infections and treatment failures. The incorporation of antibiotics into hyaluronan-cholesterol nanohydrogels (NHs) represents a novel paradigm in the delivery of therapeutic agents against intracellular bacteria. The work presented herein shows that NHs quickly enter human keratinocytes and accumulate into lysosomes. When used for targeting intracellular S. *aureus* the antimicrobial activity of loaded levofloxacin (LVF) is enhanced, possibly changing the antibiotic intracellular fate from cytosol to lysosome. Indeed, gentamicin (GM), an antibiotic that predominantly accumulates in lysosomes, showed significant and equal antibacterial activity when entrapped into NHs. These results strongly suggest that lysosomal formulations may display preferential activity towards intracellular *S. aureus*, opening new avenues for the use of HA-based NHs for treatment of such skin infections.

1. Introduction

The opportunistic pathogen *S. aureus* is a prevalent commensal organism and a significant mammalian pathogen, frequently associated with a wide range of clinical infections that include skin, soft tissues and device related infections and bacteraemia[1]. Whilst *S. aureus* is not traditionally considered as an intracellular pathogen, there is increasing evidence which suggests that this microorganism can not only invade and persist in a range of cell types[2], but also that this adaptation may offer protection from the immune response and be a factor in treatment failure due to the inability of the antibiotic/antimicrobial agent to target intracellular microorganisms. This advantageous facet of intracellular adaption is evident in intracellular pathogens such as *Mycobacteriae* which can survive and replicate within macrophages by resisting lysosomal delivery

by residing in early phase endosomal compartments[3], whilst organisms such as *Salmonellae* and *Brucellae* survive by preventing vacuole-lysosome fusion[4] and pathogens such as *Shigella spp. Listeria spp and Rickettsiae* are able to escape from phagosomes and survive into the cytosol[5]. To survive and disseminate intracellularly *S. aureus* has developed some specific adaptations; one is to resist the fusion of phagosomes with lysosomes and to multiply within the phagolysosomes of macrophages[6], whilst others, for example thought such as FnBP-dependent and -independent pathways have been shown to facilitate *S. aureus* internalization and survival within human keratinocytes[2b, 7]. Once internalized, it has been proposed that this offers protection from humoral immune responses and from the action of several antibiotics[8].

When treating an intracellular infection, a suitable antibiotic should be chosen in order to ensure drug concentration above the minimum inhibitory concentration (MIC) and in the same intracellular location as the target microorganism. Depending on their physico-chemical properties, antibiotics accumulate in various cell compartments at different concentrations; typically, weak bases tend to accumulate in membrane-bound acidic compartments, whereas weak acids are excluded from those sites[9]. Specifically, aminoglycosides[10] and macrolides[11] predominantly accumulate in lysosomes, whereas quinolones[8a, 12] accumulate in the cytosol. The β-lactams group of antibiotics[8b] have been shown to accumulate at low level within the cells (predominantly in the cytosol) likely due to their acidic character. Despite the ability of antibiotics to cross cell membrane, their intracellular efficacy can be poor due to: I) low intracellular concentrations below the minimum inhibitory value; II) intracellular environment (e.g. acidic pH) that may affect the antibiotic activity; III) antibiotic accumulation in subcellular compartments that are different from those in which pathogens persist. These limitations could potentially be overcome by utilizing suitable nano-carriers which can enhance the intracellular uptake of antibiotics[13] and facilitate the subcellular targeting[14]. Such nano-carriers can be customized in order to target lysosomes or to escape the endosome, being released into the cytosol. Indeed, carriers made of polycations can provide a

'proton sponge effect'[15] or such carriers can be conjugated to membrane-degrading/destabilizing peptides in order to break down the endosome membrane, allowing the 'cargo' release into the cytosol[16]. In this respect, a number of strategies have been studied for achieving drug delivery systems that can target specific cellular compartments[14a, 17]. Hyaluronan (HA), a generally non-toxic and non-sulphated glycosaminoglycan, is a natural component of human skin and is predominantly employed in the cosmetics industry as a dermal filler [18] or skincare agent or in viscosupplementation[18b]. A major receptor for HA is CD44, a cell-surface glycoprotein highly expressed on the surface of keratinocytes[19] and activated macrophages[20]. After binding to CD44, HA is taken up by cells and delivered to the lysosomes[21]. CD44 appears to be important in the invasion, survival and persistence of a range of microorganisms within host cells[22]. For example, *Group A Streptococcus* (GAS) has been shown to attach to epithelial cells through its HA-rich polysaccharide capsule which is reported to mediate attachment to CD44 on pharyngeal and epidermal keratinocytes[23]. Moreover, CD44 was identified as a widely distributed receptor in the epithelial tissues where colonization and infection occur and represented the major cellular receptor for the GAS entry into primary mouse keratinocytes[22b]. CD44 has also been implicated in the cellular internalization of other pathogens such as *Mycobacterium tuberculosis* in macrophages[22a] and for *Shigella spp* in epithelial cells[22d]. Consequently, the application of HA-based nano-carriers may be particularly suitable for targeting intracellular pathogens as: I) a number of host cells (e.g. keratinocytes and macrophages) highly express CD44 and easily internalize HA; II) HA can enter cells through the receptor (CD44) that is also employed by such pathogens; III) like other nanoparticles, HA nano-carriers can be engineered in order to target lysosomes or other cellular compartments[24]; IV) in the cellular micro-environment the HA nano-carriers may be cleaved by hyaluronidases (HA_{ase}) that are produced by several bacteria such as *Staphylococcus spp.* and *Streptococcus spp.*[25], facilitating the release of the drug *in situ.* Moreover, the scission of HA can also occur in the presence of host enzymes, acidic pH and free radicals[26], assuring the drug

release within the cells, thus guaranteeing the efficacy of the targeted therapy also against microorganisms that typically do not produce HA_{ase} such as *P. aeruginosa*[27] and *M. Tuberculosis*[28]. The data presented herein show the novel application of self-assembling HA-based NHs[29] for enhancing the intracellular uptake of antibiotics into human keratinocytes and targeting to intracellular *S. aureus*. The efficacy of GM or LVF versus -loaded NHs (NH/GM or NH/LVF, respectively) was explored. These two antibiotics were selected as they have different intracellular pathways: GM is a lysosomal drug[10], whilst LVF is a cytosolic one[8a]. GM is typically used in topical preparations and can be employed to treat skin infections, whilst LVF remains among the most active oral antimicrobials.

2. Results and Discussion

2.1. Development and characterization of NH/GM and NH/LVF

In order to generate NHs, HA carboxyl groups were functionalized with a small hydrophobic molecule, cholesterol (CH) [29]. In a previous work, the *soft* nature, the swelling ability, the spherical shape and size of HA-CH NHs in both dry and aqueous environments (by using Atomic Force Microscopy and Transmission Electron Microscopy techniques) were showed[30]. These nanoparticles evidenced the ability to absorb a high amount of water and to swell in aqueous media, thus showing the typical properties of NHs [31, 32]. As HA chains are chemically modified with a hydrophobic moiety (CH), the resulting amphiphilic polymer is able to self-assemble in aqueous environment and spontaneously forms physically cross-linked tri-dimensional networks which are characterized by internal hydrophobic domains and hydrophilic outer chains. Depending on the degree of functionalization and on the polymer molecular weight, these aggregates may form regular nano-structures, after suitable treatments such as sonication or autoclaving.

In this respect, it was already shown that autoclaving (121°C, 20 min) represents a fast and reproducible one-pot method for directly achieving sterile and drug-loaded NHs [33]. In this way,

both sterile NH/GM and NH/LVF were obtained after autoclaving (**Figures 1 and 2**). Nano-systems were purified from the free antibiotics using a size exclusion chromatography (SEC) column; drug loading (DL, %) and loading efficiency (LE, %) were studied with an ultra-performance liquid chromatography (UPLC) coupled with a mass-spectrometer (NH/GM) and with a UV-Vis spectrometer (NH/LVF). The amount of entrapped drug is reported in **Table 1** and shows that GM loading was higher than that of LVF; this may be due to the amino groups of the GM sugar rings, which exhibit a net positive charge under physiological conditions (pKa values of GM amine groups range from 5.6 to 9.5), establishing strong electrostatic interactions with the negatively charged HA chains. In contrast, LVF exists as a zwitterion at pH 6.0-7.5, leading to weaker interactions with NHs and, thus, lower encapsulation values. NH/GM and NH/LVF were characterized in terms of mean diameter, PDI and ζ-pot (as summarized in Figure 1A, B, C and 2A, B, C), showing average sizes of ~ 250 nm (NH/GM) and ~ 350 nm (NH/LVF). It was necessary the use of different solvents for the formulation of NH/GM and NH/LVF; pH values lower than 7 were not suitable for the formation of NH/GM as a precipitate was found after the autoclaving process (possible due to the strong electrostatic interactions occurring between GM and HA, which prevent the NHs formation by self-assembling). Whilst, less LVF was loaded into NHs at neutral pH compared to that loaded in double-distilled water (pH=5). This result can be ascribed to the zwitterionic nature of LVF. Therefore, to maximize the concentration of antibiotics loaded in the NHs a different solvent for each antibiotic was used. As expected, an increase in the amount of loaded GM led to a decrease of the ζ-pot net value of NHs (due to the positively charged GM) compared to that of the unloaded NHs. Indeed, the GM DL% of 40 ± 1%, 35.1 ± 2.8% and 30.7 ± 2% (w/w, %) led to a ζ-pot change of 49%, 24% and 20%, respectively, compared to that of free NHs, evidencing a GM concentration-dependent effect. Loaded LVF affected NHs ζ-pot to a lesser extent. Moreover, both NH/GM and NH/LVF stored at -20°C or freeze-dried as solid powders, retained their mean diameter and PDI when defrosted and re-hydrated. For preserving the starting NH/GM and NH/LVF properties, it was necessary to add dextrose before freeze-drying (Figure 1A and B). The

NHs freeze-dried powder ensures the long-term storage of the nano-formulations, as the stability of the aqueous suspensions of NHs and the loaded drugs is rather limited. The antimicrobial activity of NH/LVF freeze-dried powder was already studied against intracellular *S. aureus* and *P. aeruginosa*[27], evidencing the storage method is able to retain the whole activity of the nano-formulation. Furthermore, the NHs freeze-dried powder could be mixed with appropriate materials (e.g. carbopol), at suitable concentrations, in order to obtain formulations for topical administrations. Figs. 1 and 2 also show that liquid samples can be frozen, retaining their size and PDI and assuring a long-term storage without the addition of any additive.

Among the prepared samples, NH/GM and NH/LVF with the starting 1:1 wt. ratio (formulations written in bold in Table 1) showed the best properties and loading efficiency, therefore they were selected for subsequent experiments. To assess the stability of loaded NHs in aqueous environments, drug release studies (Figure 1D and 2D) were performed in double-distilled water (pH ~ 5 similar to that of the human skin). Results showed that only 10% (% w/w) of loaded GM was released from NHs in 24 h, evidencing the high stability of the nano-formulation. Longer time points were also checked over one week (data not shown), but no changes were observed in the release profile. This behaviour can be explained by taking into account that the electrostatic interactions between the negatively charged NHs and the positively charged GM are very strong at low ionic strength. However, some degradation mechanisms should occur in '*in vitro*' or '*in vivo*' (e.g. specific enzymes such as HA_{ase} and esterase, acidic pH and free radicals), enhancing the GM release from the NHs. In contrast, 48% (% w/w) of loaded LVF was released over 24 h in the same conditions; this result can be ascribed to weaker interactions within the NHs.

2.2. Cell viability of HaCaT

To determine the effects of antibiotics-loaded NHs on cell viability, HaCaT cells were incubated with NH/GM or NH/LVF or their antibiotic-free controls over 48 h. Both MTT (**Figure 3**A and C) and trypan-

blue (Figure 3B and D) assays showed that NHs preparations were not toxic to HaCaT, as neither HaCaT metabolism nor vitality was significantly affected by any of the tested concentrations after 48 h (Figure 3).

2.3. Antibacterial activity of NH/GM and NH/LVF against extracellular and intracellular *S.aureus*

To ensure the NHs encapsulation do not enhance or inhibit antimicrobial activity, the MIC and the minimum bactericidal concentration (MBC) of NHs alongside free GM and LVF, NH/GM and NH/LVF were determined; **figure 4**A shows the mean MIC and MBC values. Free NHs did not show any antimicrobial activity and incorporation of GM or LVF into NHs did not affect their antibacterial activity against extracellular *S. aureus*. The efficacy of the nano-formulations against intracellular *S. aureus* was then assessed by enumerating viable intracellular bacteria from infected HaCaT treated with NH/GM, NH/LVF or their controls, in conditions which did not affect the viability of HaCaT cells, by using the following concentrations: c = 46.8 μg/mL (GM) and c = 117 μg/mL (NHs) for the NH/GM system and at c = 35.1 μg/mL (LVF) and c = 307 μg/mL (NHs). Antibiotic concentrations tested were 3 fold greater than the MIC/MBC to ensure eradication of viable bacterial cells. After 2 h of incubation, NH/GM and NH/LVF and their controls were not effective against intracellular *S. aureus* (Figure 4B). After 5 h of incubation both free GM and NH/GM showed significant antimicrobial activity against the intracellular *S. aureus* ($p<0.05$); however, when compared to free GM, NHs did not enhance GM activity intracellularly. In contrast, LVF activity was highly enhanced by NHs ($p<0.005$) when compared to that of free LVF (Figure 4B).

2.4. Uptake and intracellular fate of HA-CH NHs in HaCaT

Rhodamine B-isothiocyanate (rhod) dye was covalently linked to the hydroxyl groups of NHs and the obtained fluorescent NHs were employed for studying their binding/internalization kinetics and

intracellular fate into HaCaT by flow cytometry and fluorescence microscopy. Flow cytometry analysis evidenced that HaCaT incubated for 30 min with rhod-NHs showed a significant increase in fluorescence intensity, indicating a quick binding/uptake of NHs within the cells. HaCaT fluorescence steadily increased over the time and 4 h represented the time point at which the highest signal was detected, followed by a plateau up to 24 h (**Figure 5**A). Moreover, HaCaT cells showed increased fluorescence in a dose-dependent manner with rhod-NHs concentrations up to 100 µg/mL after 4 h of incubation (Figure 5B).

ApoTome analysis showed NHs located into vesicle-like structures, those with a diameter of approximately 0.3 µm close to the plasma membrane and those in larger vesicles with diameter up to 1.5 µm close to the nucleus, suggesting an intracellular location of NHs (**Figure 6**). Interestingly, Tammi et al. (2001) had a similar outcome using free HA in rat epidermal keratinocytes [19a]. To determine the intracellular fate of NHs and explore the possibility of their co-localization with lysosomes, HaCaT were then incubated up to 24 h with the nano-system and stained with 'Lyso-tracker Green DND-26' (**Figure 7**). At 1 h a limited number of NHs was located in lysosomes; however, from 4 to 24 h a strong co-localization occurred (***P value < 0.005) compared to that at 1 h, showing the highest Pearson correlation coefficient value [34] (0.94) at 4 h. NHs in lysosomes were still evident up to 24 h, although co-localization was weaker than that found at 4 h (~ 0.7) (Figure 7); no significant differences were found in the time points ranging from 6 to 24 h.

Since a previous work showed that LVF predominantly accumulates in the cytosol, it is plausible that NHs are able to change the intracellular fate of LVF (from cytosol to lysosome), delivering the antibiotic to the intracellular location of *S. aureus* (**Figure 8**), thus enhancing its intracellular antimicrobial activity (Figure 4B). On the other hand, GM, an antibiotic that predominantly accumulates in lysosomes, showed a significant antibacterial activity without the presence of NHs. These results strongly suggest that therapeutics that are able to accumulate in lysosomes might be more effective against intracellular *S. aureus* compared with those that accumulate in other cell

compartments (e.g. cytosol), evidencing that: I) sub-cellular targeting could be necessary for eradicating the intracellular pathogen; II) lysosomal nanoparticles (e.g. HA-CH NHs) might be suitable for enhancing the antibacterial activity of such antibiotics against the intracellular *S. aureus* in human keratinocytes.

3. Conclusion

We have shown that self-assembled NHs can be loaded with GM or LVF antibiotics by means a fast one-step sterile cycle using an autoclave (121°C for 20 min). NH/GM and NH/LVF show mean diameters of approximately 250 and 350 nm, respectively; both nano-formulations do not affect viability of HaCaT cells at all tested concentrations over 48 h and display the same MIC and MBC values as free antibiotics against extracellular *S. aureus*. However, intracellularly, the antibacterial activity of LVF was highly enhanced by NHs. As we have demonstrated that NHs co-localize with lysosomes of HaCaT cells and it is known that free LVF predominantly accumulates in the cytosol, these results strongly suggest that NHs may be able to change the intracellular fate of LVF from cytosol to lysosome, thereby targeting intracellular *S. aureus*. Indeed, GM, an antibiotic that predominantly accumulates in lysosomes, shows significant intracellular activity without the employment of NHs. To conclude, this research demonstrates that lysosomal formulations may be more effective against *S. aureus* in keratinocytes compared with formulations that accumulate in other cell compartments (e.g. cytosol), opening new avenues for HA-based NHs treatments of persistent *S. aureus* skin infections.

4. Experimental section

Materials: Hyaluronan tetrabutylammonium salt (HA^-TBA^+, M_w = 2.2 x 10^5) was purchased from Contipro (Dolní Dobrouč, Czech Republic). Cholesterol (CH), 4-bromobutyric acid, N-methyl-2-pyrrolidone (NMP), N-(3-dimethylaminopropyl)-N′-(ethylcarbodimide hydrochloride) (EDC·HCl), gentamicin sulfate (GM), levofloxacin (LVF), 4-(dimethylamino)pyridine (DMAP), phosphate

buffered saline tablets, dextrose, dimethyl sulfoxide ACS reagent ≥99,9%, trypsin-EDTA solution 10X, formaldehyde solution for molecular biology ≥36.0%, 4',6-diamidino-2-phenylindole dilactate (DAPI) for nuclei staining, Mowiol® 4-88, rhodamine B isothiocyanate, Hanks' Balanced Salt solution (HBSS) and L-glutamine were purchased from Sigma-Aldrich (Milan, Italy). Dulbecco's Modified Eagle Medium (DMEM 1X) was purchased from Gibco® brl life technologies™ inc., Grand Island (NY, USA). Lyso-Tracker Green DND-26, Invitrogen™ Molecular probes® were purchased from Thermo Fisher Scientific (Monza, Italy). Triton® X-100, albumin from bovine serum, ammonium formate, trypan blue solution were purchased from Biochemica Fluka, Sigma-Aldrich (Milan, Italy). Nitrotetrazolium blue chloride (MTT, CellTiter 96® Non-Radioactive Cell Proliferation Assay) was purchased from Promega (Milan, Italy). Acetonitrile for HPLC and ACS water suitable for UPLC/UHPLC instruments were purchased from VWR (Milan, Italy).

Bacterial strains: Staphylococcus aureus NCTC 12973 was obtained from Public Health England Southampton, UK. Stock cultures were stored at -80°C using Protect cryobead vials (Technical Service Consultants Ltd, Heywood UK). Prior to experiments bacterial cultures were revived by transferring cryobead/s onto fresh sterile Mueller-Hinton agar and incubated at 37°C for 24 h. Dehydrated bacteriological media were obtained from Oxoid (Basingstoke, Hampshire, U.K.) and reconstituted according to the manufacturer's instructions. Bacterial growth media were sterilized at 121°C, 15 psi for 15 min prior to use.

General cell culture: The human keratinocyte cell line (HaCaT) was spontaneously immortalized from primary keratinocytes[35] and cultured in high glucose Dulbecco's Modified Eagle's Medium (DMEM; EuroClone, Milan, Italy) supplemented with 10% (v/v) fetal bovine serum (FBS) and 4 mM glutamine at 37°C in a humidified atmosphere with 5% CO_2. Cells were grown to 70-80% semi-confluence, according to each experimental setting and treated with free or loaded antibiotics at several time points and concentrations. All experiments contained untreated cells (PBS) processed in parallel as negative control.

Synthesis of cholesterol-Br-butyric derivative (CH-Br): CH-Br synthesis was carried out as previously described [29]. Briefly, 500 mg of CH (1.3 x 10^{-3} mol) were solubilized in 5 mL of CH_2Cl_2 and added to 79 mg of DMAP (6.5 x 10^{-4} mol); the solution was stirred for 15 min at 25°C. Meanwhile, 648 mg of 4-bromobutyric acid (3.9 x 10^{-3} mol) and 744 mg of EDC·HCl (3.9 x 10^{-3} mol) were solubilized in 5 mL of CH_2Cl_2; the two solutions were then mixed and kept at 25°C with magnetic stirring, overnight. Reaction products were checked with silica gel TLC (cyclohexane : ethylacetate, 85:15) and then washed once with 50 mM NaOH and HCl and three times with bi-distilled water. The solution was firstly dried with anhydrous Na_2SO_4 and then with vacuum evaporation. The crude product (powder) was finally purified with a silica column (eluent, cyclohexane : ethylacetate, 98.5:1.5); 310 mg of pure CH-Br were obtained (yield 60%, % w/w).

Synthesis of hyaluronan-cholesterol amphiphilic polymer (HA-CH): HA-CH synthesis was carried out as previously reported [29]. 200 mg of HA^-TBA^+ (M_w = 2.2 x 10^5) were added to 10 mL of NMP and the sample was kept at 25°C for 5 h with magnetic stirring; then, 34.3 mg of CH-Br, previously solubilized in 2 mL of NMP, were added and the reaction was allowed to proceed for 48 h at 38°C with magnetic stirring. Then, 2 mL of NaCl (saturated solution) were added to the polymer solution and the mixture was left under stirring for 30 min to allow the exchange of the Na^+ with TBA^+ ions. The reaction product was precipitated in acetone (4 times the reaction volume), left for 1 h at 4°C, isolated, re-suspended in bi-distilled water and finally dialysed against water (cellulose membrane tubing, Mw cut-off: 1.2-1.4 x 10^4, Sigma-Aldrich, Darmstadt, Germany) until constant conductivity was reached. Sample was freeze-dried with a "Modulyo 4K" Edwards High Vacuum instrument, equipped with an Edwards pump, operating at 0.2 atm and at −40°C, yielding 354 mg of white solid (71% mass recovery). Theoretical degree of functionalisation (DF) was 15% (% mol/mol, corresponding to mol of CH per mol of HA repeating unit).

Preparation and characterization of GM or LVF-loaded HA-CH nanohydrogels (NH/GM or NH/LVF): 2 mg of HA-CH were dispersed in 1 mL of Milli-Q water (2 mg mL^{-1}) overnight with magnetic stirring at 25°C. Then 1 mL PBS (pH=7.4) and 0.1 mL of GM solution (10, 5 or 2.5 mg mL^{-1}), or 1 mL Milli-Q water and 0.1 mL of LVF solution (10, 5 or 2.5 mg mL^{-1}) (corresponding to 1:1, 1:0.5 and 1:0.25 HA-CH:GM or HA-CH:LVF wt. ratio) were added. Samples were then autoclaved for 20 min at 121°C, leading to NH/GM or NH/LVF formation. NH/GM or NH/LVF ~~suspensions~~ were purified from the free antibiotics through SEC. SEC was performed using Econo-Pac chromatography columns (Bio-Rad, Segrate, Italy) packed with Bio-Gel® P-10 (polyacrylamide with an exclusion limit range of 1.5-20 x 10^3, Bio-Rad, Segrate, Italy). 1 mL of NH/GM or NH/LVF mixtures was loaded into SEC and eluted with 10 mL PBS or water, respectively, at 25°C and atmospheric pressure.

Dynamic Light Scattering (DLS): hydrodynamic diameter (Z-average size), size distribution, polydispersity (PDI), and ζ-potential of NH/GM or NH/LVF were measured by Dynamic Light Scattering (DLS) at 25 °C by using a Zetasizer Nano ZS instrument (Model ZEN3690, Malvern Instruments) equipped with a solid state HeNe laser (λ = 633 nm) at a scattering angle of 173°. Size measurement data were analyzed by using the general purpose algorithm. The electrophoretic mobility of the samples was converted in ζ-potential by using the Smoluchowski equation. Hydrodynamic diameter and PDI of freeze-thawed or freeze-dried NH/GM or NH/LVF were also studied; empty NHs were prepared as controls. Each experiment was performed in triplicate (n=3).

Quantification of entrapped GM or LVF into NHs:

A) *UPLC coupled to mass spectrometry (LC-MS) analysis*: the amount of GM entrapped into NHs was checked with a Waters Acquity H-Class UPLC liquid chromatography-mass spectrometer (Waters, Milford, MA, USA), equipped with a quaternary solvent manager (QSM), a sample

manager with flow through needle system (FTN) and a single-quadrupole mass detector with electrospray ionization source (ACQUITY QDa). Free GM solutions were diluted with water, filtered with 0.22 µm regenerated cellulose membrane filters (Sartorius Italy s.r.l., Monza, Italy) and injected into a Waters BEH Shield C18 column (50 mm × 2.1 mm i.d., 1.7 µm particle size). Samples were eluted using an isocratic 10 mM $HCOONH_4$ mobile phase (pH = 3) at a flow rate of 0.5 mL min^{-1} and column temperature of 25°C. Mass spectrometry detection was performed in positive electrospray ionization mode (ESI), using nitrogen as nebulizer gas. Three m/z values (478, 464 and 450) corresponding to the three $[M+H]^+$ GM chemical species were monitored in single ion recognition mode (SIR). Capillary and cone voltage were set to 0.8 kV and 15 V; ion source and probe temperatures were adjusted to 120°C and 600°C. A GM calibration curve was calculated at the concentration range of 7.5-125 µg mL^{-1} (R^2 = 0.98, n= 3).

B) *UV-Vis spectrometry analysis:* the amount of LVF entrapped into NHs was assessed by using a Perkin-Elmer double beam "Lambda 3A" model. Analyses were performed at 25°C, using 1 mm quartz cuvettes (Hellma Analytics, Milan, Italy). LVF water solutions were detected at 286 nm. A LVF calibration curve was built at the concentration range of 16-200 µg mL^{-1} (R^2 = 0.999, n=5). The amount of entrapped GM or LVF was calculated by subtracting the amount of unloaded GM or LVF from the starting total amount of drugs. Each experiment was performed in triplicate (n=3).

Drug loading (DL%) and loading efficiency (LE%) of both GM and LVF were calculated using the following equation (1) and (2):

$$DL\% = \frac{weigh\ \ of\ loaded\ drug}{weig\ \ \ of\ total\ drug}\ x\ 100 \qquad (1)$$

$$LE\% = \frac{wei \quad of\ loaded\ drug}{weight\ of\ polymer}\ x\ 100 \qquad (2)$$

In vitro release studies of GM or LVF from NHs: 1 mL of purified NH/GM or NH/LVF (1:1 starting wt. ratio) was put into a membrane tube (Mw cut-off 1.2-1.4 x 10^4) and dialysis was performed against 15 mL bi-distilled water for 24 h, at 37°C; at specific time points 3 mL solution were taken off and replaced with 3 mL of bi-distilled water. Samples were then injected into UPLC-MS or analysed with UV-Vis spectrometer for quantifying the amount of released GM or LVF from NHs, respectively. Each experiment was performed in triplicate (n=3).

Cell viability assays: HaCaT viability was tested in parallel with 3-(4,5-dimethylthiazol-2-yl)-2,5-diphenyltetrazolium bromide metabolic assay (MTT assay) and trypan blue exclusion method, by counting both dead and living cells.

A) *MTT test:* 100 µL HaCaT (5,000 cells/well in complete DMEM) were seeded in a 96-well plate (Falcon™ Polystyrene Microplates, Thermo Fisher Scientific, Monza, Italy) and incubated for 24 h. Cell monolayers were then added to 25 µL of samples (free NHs, GM or LVF, NH/GM or NH/LVF in PBS pH=7.4) at specific final NHs concentrations (ranging from 18-500 and 37-1000 µg mL^{-1} for NH/GM and NH/LVF respectively, df: 1:3) and incubated for 24 and 48 h. As negative control, cells received 25 µL PBS. Then, medium was removed, cells were gently washed with PBS and 100 µL complete DMEM were added. 20 µL MTT solution (Promega, Italy, Milan) were added and HaCaT were incubated for 2 h. Supernatants were gently removed and formazan crystals were solubilised with 100 µL DMSO. Absorbance was checked at 570 nm with a reference at 690 nm, using an Appliskan microplate reader (Thermo Scientific, Vantaa, Finland). Each experiment was performed on sixteen wells (n=3). Results were processed using SkanIt 2.3 Software.

B) *Trypan Blue exclusion method:* 1.5 mL HaCaT (167,000 cells/well in completed DMEM) were seeded in a 6-well plate and incubated for 24 h. 0.375 mL of free NHs or NH/GM or NH/LVF in PBS at the final NHs concentration of 500 or 1000 µg mL^{-1} (NH/GM or NH/LVF respectively) were then added to the cells, which were incubated for 24 and 48 h. As negative control, cells received 0.375 mL PBS. Subsequently, medium (1.875 mL) was taken off and stored into eppendorf tubes (Primo® boil-proof microcentrifuge tubes, EuroClone spA, Milan, Italy); then, wells were gently washed with 1 mL PBS and 0.6 mL 0.5% trypsin were added. Cells were allowed to detach for 10 minutes at 37°C and then added to the previously removed 1.875 mL DMEM. 80 µL cell suspensions were mixed with 80 µL 0.4% trypan blue solution and cells were counted with a Primovert microscope (Carl Zeiss Microimaging GmbH, Gottingen, Germany) in a Neubauer chamber. Each experiment was performed in triplicate (n=3).

Determination of MICs and MBCs:

The MIC and MBC were determined for axenic planktonic populations of *S. aureus* using the microdilution method [36]. Briefly, 100 µL double strength Mueller-Hinton broth was dispensed in wells of the first column of a flat bottom 96-well microtiter plate. Stationary phase cultures of *S. aureus* grown in Mueller-Hinton broth, were adjusted in fresh sterile Mueller-Hinton broth to give a cell density of c. 2 x 10^6 CFU mL^{-1}. Within 30 minutes of preparation inocula were dispensed (100 µL) into the remaining wells the 96-well plate. Stock solutions of free GM, LVF, NHs or NH/GM or NH/LVF were prepared in sterile PBS and dispensed (100 µL) into the first column of the microtiter plate. Doubling dilutions of samples were then undertaken across the plate (100 µL). Plates were incubated at 37°C for 24 h. The MIC endpoint was determined as the lowest concentration of antimicrobial that prevented visible growth. To determine the MBC, aliquots (10 µL) from wells exhibiting no turbidity were spot plated onto sterile Mueller-Hinton agar. After incubation at 37°C,

the MBC endpoint was determined as the lowest concentration that resulted in no visual growth of colonies after 24 h of incubation. Each experiment was performed in triplicate (n=3).

Cell infection and assessment of intracellular activity of NH/GM or NH/LVF: To assess the efficacy of free or loaded GM or LVF on intracellular bacteria, HaCaT cell monolayers were grown to 70-80% semi-confluence by seeding 1.5 x 10^5 cells in 1 mL of complete DMEM (2 mM glutamine) in 24-well plates and incubating for 18 h. Mid-log phase cultures of *S. aureus* were washed twice with sterile PBS and culture densities adjusted in sterile, FCS free DMEM to give a cell density of c. 100 CFU/cell (100 MOI). Growth medium was removed and HaCaT cells were washed with sterile PBS and FCS free medium was added to each well. Aliquots of adjusted bacterial cultures were added to cells and plates were incubated for a further 3 h. In order to remove any extracellular bacteria, cell culture media were then removed from wells and 1 mL fresh serum free media containing X2 MIC gentamicin added. Plates were further incubated for 1 h. Medium was removed and HaCaT cells were washed twice with sterile PBS. Free GM or LVF and their nano-formulations were reconstituted in sterile PBS and diluted to the desired concentration in fresh serum free DMEM in order to have 3X MIC value (final concentration of drugs in the well). 1 mL aliquots of treatments were then added to cells and plates were incubated for either 2 or 5 h. After incubation, cells were washed twice with PBS and lysed with 0.025% Triton X for 10 min. To enumerate viable bacteria, lysates were harvested and serially diluted in sterile PBS and inoculated onto Mueller-Hinton agar. Agar plates were incubated for > 16 h and viable counts performed. All experiments contained non-infected cell monolayers processed in parallel as a sterile control and infected cell monolayers processed with serum free media in the absence of any test treatment as a positive control. Each experiment was performed in triplicate (n=3).

Synthesis of fluorescent NHs (rhod-NHs): 1.5 mg mL^{-1} HA-CH polymer in bi-distilled water was left with magnetic stirring overnight at 25°C. The sample was placed in an autoclave (121°C for 20 min) where NHs were allowed to form. Rhodamine B-isothiocyanate (rhod) was previously solubilized in DMSO at a concentration of 9 mg mL^{-1} and then added to NHs suspension (8 µL for 1 mg of polymer, corresponding to a DF of 6.3%; % mol/mol). The reaction mixture was left for 5 h at 25°C in the dark, following which it was dialysed against water until constant conductivity was reached and then freeze-dried. The final DF% was assessed through UV-Vis analysis: sample was solubilized in DMSO and checked at 550 nm at 25°C. A rhod calibration curve was built at the concentration range of 8.5-125 µg mL^{-1} in DMSO. DF corresponded to 1.3% (mol of rhod per mol of HA-CH repeating unit).

Flow cytometry analysis: Cell binding/uptake kinetics of fluorescent NHs was studied with a BD Accuri C6, BD 254 Biosciences (Erembodegem, Belgium) flow cytometer equipped with a 488 nm excitation laser and a 585/40 nm band-pass filter (FL2 channel). For each sample 50,000 events were collected. 1 mL HaCaT cell suspension (67,000 cells/well in complete DMEM) was seeded in 12-well plates and incubated for 48 h. Cells were washed three times with PBS, 1.5 mL of complete DMEM added and treated with 0.25 mL of 0.5 mg mL^{-1} rhod-NHs in PBS (corresponding to a final concentration of 0.10 mg mL^{-1}) at specific time points, over 24 h. Medium was removed, cells were washed three times with PBS, allowed to detach with 0.25 mL trypsin and finally added to 0.75 mL complete DMEM. Cell suspensions were centrifuged in eppendorf tubes for 8 min at 1,200 rpm at 4°C. Supernatants were removed and pellets were washed with 1 mL HBSS solution and centrifuged again. Pellets were re-suspended in 0.5 mL HBSS and red fluorescence (rhod) was detected with a flow cytometer. HaCaT cells were also treated with 0.25 mL of rhod-NHs (final concentrations 10, 50, 100, 500 µg mL^{-1}) at a fixed time point (4 h) by following the same procedure and then analysed with a flow cytometer. As a negative control, cells received 0.25 mL PBS. Results are expressed as median fluorescence intensity. (n=3). A dot plot was built by plotting Forward scatter (FSC-H) versus

Side scatter (SSC-H) and the gate was constructed excluding cell debris. Each experiment was performed in triplicate (n=3).

Cell imaging:

ApoTome microscope: Immunofluorescence signal of fluorescent NHs was analysed by recording stained images using an Axio Observer Z1 inverted microscope, equipped with an ApoTome.2 System (Carl Zeiss Inc., Ober Kochen, Germany). The ApoTome system provides an optical section of fluorescent samples, calculated from three images with different grid positions without time lag. Digital images were acquired with the AxioCam MRm high resolution digital camera (Zeiss) and processed with the AxioVision 4.8.2 software (Zeiss). ApoTome optical sectioning images of fluorescent NHs were recorded under 40x/0.75 objective (Zeiss). Pearson's correlation coefficient [32] was used to quantify the degree of colocalization between fluorescent NHs and Lyso-Tracker Green DND-26 staining in a series of 0.5 nm sequential sections, under an immersion oil 63x/1.25 objective (Zeiss). Pearson's correlation coefficient was calculated using the AxioVision 4.8.2 software (Zeiss), analyzing a minimum of 40 cells randomly taken from each slide from three independent experiments. Images were obtained from the 2D reconstruction of selected serial optical sections.

Cellular uptake micro-graphs: 1.5 mL HaCaT cells (167,000 cells/well in complete DMEM) were seeded on microscope slides (Prestige micro cover glass 22 X 22 mm, Syntesys Disposable Labware, Padova, Italy) in a 6-well plate and allowed to adhere for 48 h. Then, cells were washed three times with PBS, 1.5 mL of complete DMEM added and incubated with 0.375 mL of 0.5 mg mL^{-1} rhod-NHs in PBS (corresponding to a final concentration of 0.1 mg mL^{-1}) or free rhod previously solubilised in DMSO (final concentration of 7.2 µg mL^{-1}). After 4 h, medium was removed and cells were washed three times with PBS. Cells were fixed with 2% (v/v) formaldehyde (2 mL, 10 min), washed three

451 times with PBS and incubated with Triton X-100 (0.1%, v/v, 2 mL, 5 min). Cells were washed three
452 times with PBS and nuclei were stained with DAPI reagent (1 µg mL^{-1}, 1 mL for 1 min). Finally, cells
453 were washed again and 8 µL Mowiol were added; slides were allowed to dry and fix overnight at
454 25°C on StarFrost® microscope slides (Braunschweig, Germany). Samples were then analysed with
455 the ApoTome microscope.
456
457 *Lysosomal co-localization in living cells:* 1.5 mL HaCaT (167,000 cells/well in complete DMEM) were
458 seeded on microscope slides in a 6-well plate and allowed to adhere for 48 h. Cells were washed
459 three times with PBS, 1.5 mL of complete DMEM added and incubated with 0.375 mL of 0.5 mg mL^{-1}
460 rhod-NHs (corresponding to a final concentration of 0.1 mg mL^{-1}). After several time points (from
461 0.5 to 24 h) slides were washed three times with PBS, 1.5 mL of complete DMEM added and finally
462 incubated with 1 mL of Lyso-Tracker Green DND-26 staining (final concentration of 200 nM) for 3
463 min at 37°C. Images were immediately recorded on living cells with the ApoTome microscope.
464 Results were obtained from three independent experiments, each derived from eight images.
465
466 *Statistical analysis:*
467 *Cell infection and assessment of intracellular activity of NH/GM or NH/LVF.*
468 Viable cell counts were calculated using three biological replicate count data (each derived from
469 three technical replicate data). All data were Log10 transformed and are expressed as the mean
470 value ± standard deviation. Statistical significance was determined using biological replicate data
471 (n=3) with Mann-Whitney test by using SPSS 20 Software. P values < 0.05 were considered
472 significant. Asterisk denote statistically significant differences (*P<0.05).
473 *Cell viability and cell count assays*
474 Viable HaCaT (MTT and trypan blue) were calculated using three biological replicates (each derived
475 from sixteen wells). Cell viability and cell growth were normalized to the negative control (untreated

cells that received PBS), whilst the cell death was normalized to the total amount of cells. All data are expressed as the mean value ± standard deviation. Statistical significance was determined using sixteen wells (n=3) with One-way ANOVA analysis in Prism (GraphPad 5.0 Software, Inc., La Jolla, CA, USA). Differences between groups were determined by a Turkey's multiple comparison test. Asterisks denote statistically significant differences (*P<0.05; **P<0.01; ***P<0.005).

Co-localization experiments

Pearson's correlation coefficient was used to quantify the degree of co-localization between fluorescent NHs and Lyso-Tracker Green DND-26 staining, which was calculated using the AxioVision 4.8.2 software (Zeiss) and expressed as the mean value ± standard deviation. Results were obtained from three independent experiments, each derived from eight images. Statistical significance was determined using One-way ANOVA analysis.

Graphs and Figures: All graphs and figures were processed with OriginPro 2016 and CorelDraw Graphics Suite X8 Softwares.

Acknowledgments

The authors acknowledge financial support from Sapienza University of Rome ("Finanziamenti di Ateneo per la Ricerca Scientifica - RP116154C2EF9AC8" and "Progetto di Ricerca RM11715C1743EE89".). The authors want also to thank Georgiana Cercelaru for her contribution in cell culture.

References

[1] a) T. J. Foster, *Nat. Rev. Microbiol.* **2005**, *3*, 948; b) L. S. Miller, J. S. Cho, *Nat. Rev. Immunol.* **2011**, *11*, 505.

[2] a) M. Kubica, K. Guzik, J. Koziel, M. Zarebski, W. Richter, B. Gajkowska, A. Golda, A. Maciag-Gudowska, K. Brix, L. Shaw, T. Foster, J. Potempa, *PLOS ONE* **2008**, *3*, 1409; b) S. Kintarak, S. A. Whawell, P. M. Speight, S. Packer, S. P. Nair, *Infect. Immun.* **2004**, *72*, 5668.

[3] J. Pieters, *Microbes Infect.* **2001**, *3*, 249.

[4] a) A. Richter-Dahlfors, A. M. J. Buchan, B. B. Finlay, *J. Exp. Med.* **1997**, *186*, 569; b) S. Köhler, F. Porte, V. Jubier-Maurin, S. Ouahrani-Bettache, J. Teyssier, J.-P. Liautard, *Vet. Microbiol.* **2002**, *90*, 299.

[5] a) T. Suzuki, C. Sasakawa, *Infect. Immun.* **2001**, *69*, 5959; b) D. A. Portnoy, V. Auerbuch, I. J. Glomski, *J. Cell Biol.* **2002**, *158*, 409; c) L. S. Van Kirk, S. F. Hayes, R. A. Heinzen, *Infect. Immun.* **2000**, *68*, 4706.

[6] a) R. S. Flannagan, B. Heit, D. E. Heinrichs, *Cell. Microbiol.* **2016**, *18*, 514; b) G. B. Mackaness, *J. Exp. Med.* **1960**, *112*, 35.

[7] A. Haggar, M. Hussain, H. Lönnies, M. Herrmann, A. Norrby-Teglund, J.-I. Flock, *Infect. Immun.* **2003**, *71*, 2310.

[8] a) C. Seral, M. Barcia-Macay, M. P. Mingeot-Leclercq, P. M. Tulkens, F. Van Bambeke, *J. Antimicrob. Chemoth.* **2005**, *55*, 511; b) F. Van Bambeke, J. M. Michot, P. M. Tulkens, *J. Antimicrob. Chemoth.* **2003**, *51*, 1067.

[9] S. Carryn, H. Chanteux, C. Seral, M.-P. Mingeot-Leclercq, F. Van Bambeke, P. M. Tulkens, *Infect. Dis. Clin.*, *17*, 615.

[10] M. Maurin, D. Raoult, *Antimicrob. Agents Ch.* **2001**, *45*, 2977.

[11] K. Falzari, Z. Zhu, D. Pan, H. Liu, P. Hongmanee, S. G. Franzblau, *Antimicrob. Agents Ch.* **2005**, *49*, 1447.

[12] M. Barcia-Macay, C. Seral, M.-P. Mingeot-Leclercq, P. M. Tulkens, F. Van Bambeke, *Antimicrob. Agents Ch.* **2006**, *50*, 841.

[13] M.-H. Xiong, Y. Bao, X.-Z. Yang, Y.-H. Zhu, J. Wang, *Adv. Drug Deliv. Rev.* **2014**, *78*, 63.

[14] a) L. Rajendran, H.-J. Knölker, K. Simons, *Nat. Rev. Drug Discov.* **2010**, *9*, 29; b) R. A. Petros, J. M. DeSimone, *Nat. Rev. Drug Discov.* **2010**, *9*, 615.

[15] a) J.-P. Behr, *CHIMIA Int. J. Chem.* **1997**, *51*, 34; b) N. M. Zaki, A. Nasti, N. Tirelli, *Macromol. Biosci.* **2011**, *11*, 1747.

[16] a) M. Lakadamyali, M. J. Rust, X. Zhuang, *Microbes infect.* **2004**, *6*, 929; b) E. Wagner, *Adv. Drug Deliv. Rev.* **1999**, *38*, 279.

[17] A. L. Armstead, B. Li, *Int. J. Nanomed.* **2011**, *6*, 3281.

[18] a) Y. Zhu, C. Crewe, P. E. Scherer, *Sci. Trans. Med.* **2016**, *8*, 323; b) A. Fakhari, C. Berkland, *Acta Biomater.* **2013**, *9*, 7081.

[19] a) R. Tammi, K. Rilla, J.-P. Pienimäki, D. K. MacCallum, M. Hogg, M. Luukkonen, V. C. Hascall, M. Tammi, *J. Biol. Chem.* **2001**, *276*, 35111; b) D. L. Hudson, J. Sleeman, F. M. Watt, *J. Cell Sci.* **1995**, *108*, 1959.

[20] a) C. B. Underhill, H. A. Nguyen, M. Shizari, M. Culty, *Dev. Biol.* **1993**, *155*, 324; b) J. M. Rios de la Rosa, A. Tirella, A. Gennari, I. J. Stratford, N. Tirelli, *Adv. Healthc. Mater.* **2017**, *6*, 1601012-n/a.

[21] R. Racine, M. E. Mummert, InTech, Rijeka, **2012**, 14.

[22] a) J. C. Leemans, S. Florquin, M. Heikens, S. T. Pals, R. v. d. Neut, T. van der Poll, *J. Clin. Inv.* **2003**, *111*, 681; b) C. Cywes, I. Stamenkovic, M. R. Wessels, *J. Clin. Inv.* **2000**, *106*, 995; c) F. L. Moffat, T. Han, Z.-M. Li, M. D. Peck, R. E. Falk, P. B. Spalding, W. Jy, Y. S. Ahn, A. J. Chu, L. Y. W. Bourguignon, *J. Cel. Physiol.* **1996**, *168*, 638; d) A. Skoudy, J. Mounier, A. Aruffo, H. Ohayon, P. Gounon, P. Sansonetti, G. Tran Van Nhieu, *Cell. Microbiol.* **2000**, *2*, 19.

[23] H. M. Schrager, S. Albertí, C. Cywes, G. J. Dougherty, M. R. Wessels, *J. Clin. Inv.* **1998**, *101*, 1708.

[24] a) L. Contreras-Ruiz, M. de la Fuente, J. E. Párraga, A. López-García, I. Fernández, B. Seijo, A. Sánchez, M. Calonge, Y. Diebold, *Mol. Vis.* **2011**, *17*, 279; b) C.-S. Lee, K. Na, *Biomacromolecules* **2014**, *15*, 4228.

[25] W. L. Hynes, S. L. Walton, *FEMS Microbiol. Lett.* **2000**, *183*, 201.

[26] R. Stern, G. Kogan, M. J. Jedrzejas, L. Šoltés, *Biotechnol. Adv*., **2007**, *25*, 537.

[27] E. Montanari, G. D'Arrigo, C. Di Meo, V. Virga, T. Coviello, C. Passariello, P. Matricardi, *Eur. J. Pharm. Biopharm*. **2014**, *87*, 518.

[28] J. P. Silva, C. Gonçalves, C. Costa, J. Sousa, R. Silva-Gomes, A. G. Castro, J. Pedrosa, R. Appelberg, F. M. Gama, *J. Control. Rel.* **2016**, *235*, 112.

[29] E. Montanari, S. Capece, C. Di Meo, M. Meringolo, T. Coviello, E. Agostinelli, P. Matricardi, *Macromol. Biosci.* **2013**, *13*, 1185.

[30] E. Montanari, C. Di Meo, S. Sennato, A. Francioso, A. L. Marinelli, F. Ranzo, S. Schippa, T. Coviello, F. Bordi, P. Matricardi, *New Biotechnol.* **2017**, *37*, 80.

[31] S. V. Vinogradov, E. Batrakova, A. V. Kabanov, *Colloid Surf. B-Biointerfaces* **1999**, *16*, 291.

[32] K. Akiyoshi, S. Deguchi, N. Moriguchi, S. Yamaguchi, J. Sunamoto, *Macromolecules* **1993**, *26*, 3062.

[33] E. Montanari, M. C. De Rugeriis, C. Di Meo, R. Censi, T. Coviello, F. Alhaique, P. Matricardi, *J. Mat. Sci.: Mat. Med.* **2015**, *26*, 32

[34] V. Zinchuk, Y. Wu, G. Zinchuk, *Sci. Rep.* **2013**, *3*, 1365.

[35] P. Boukamp, R. T. Petrussevska, D. Breitkreutz, J. Hornung, A. Markham, N. E. Fusenig, *J. Cell Biol.* **1988**, *106*, 761.

[36] J. M. Andrews, *J. Antimicrob. Chemother.* **2001**, *48*, 5.

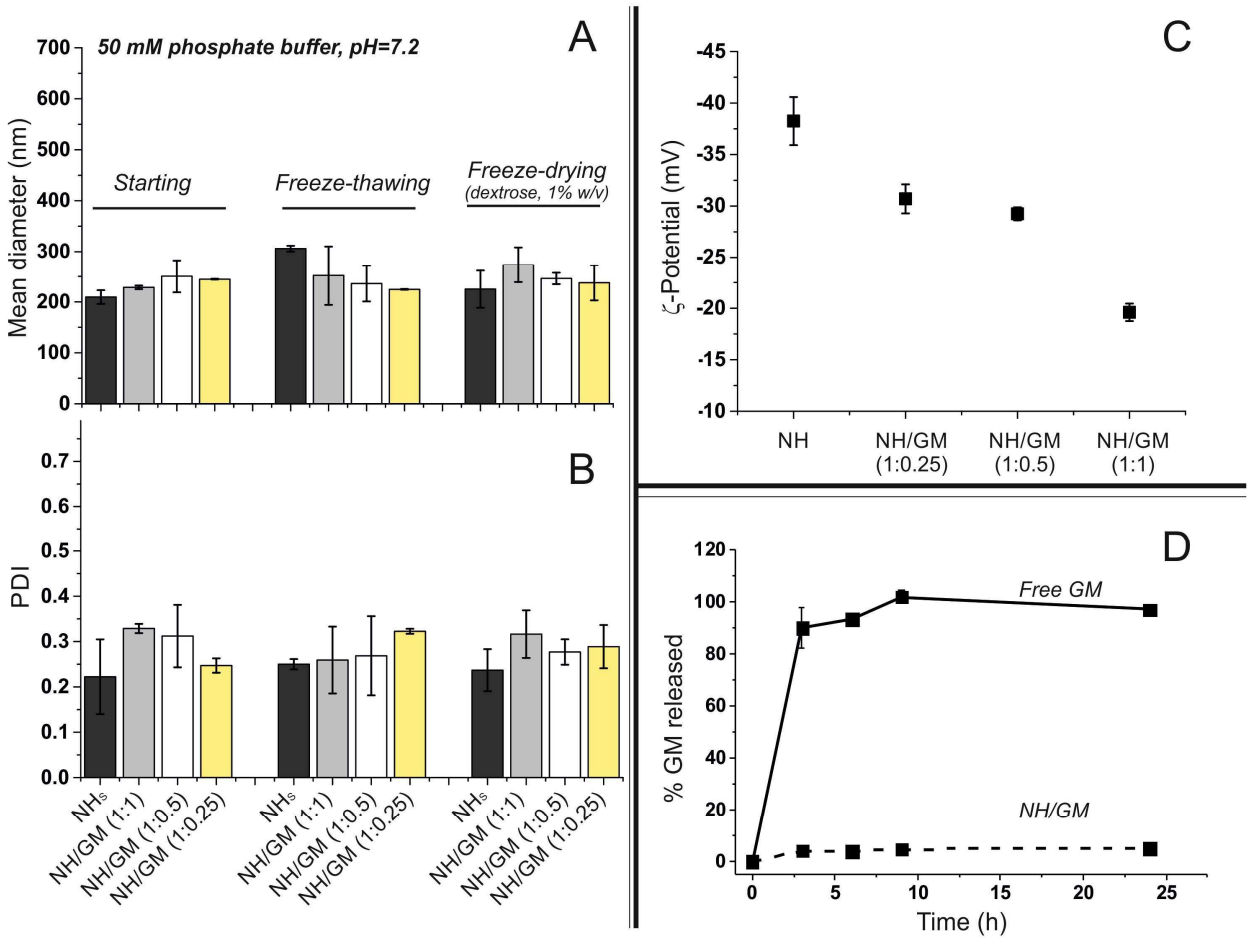

Figure 1. Mean diameter (A) and PDI (B) of starting, freeze-thawed and freeze-dried NH/GM. HA-CH/GM mixtures were prepared at several wt. ratios (ranging from 1:0.25 to 1:1 of HA-CH and GM, respectively) in 50 mM PBS (pH=7.4)

and then autoclaved at 121°C for 20 min. Unloaded GM was discarded by purification through a SEC column. (C) ζ-pot of NH/GM samples. (D) Release of GM from NHs over 24 h at 37°C in bi-distilled water. Released GM was analysed though UPLC coupled with mass-spectrometer. All data are expressed as the mean value ± standard deviation. Results were obtained in triplicate (n=3).

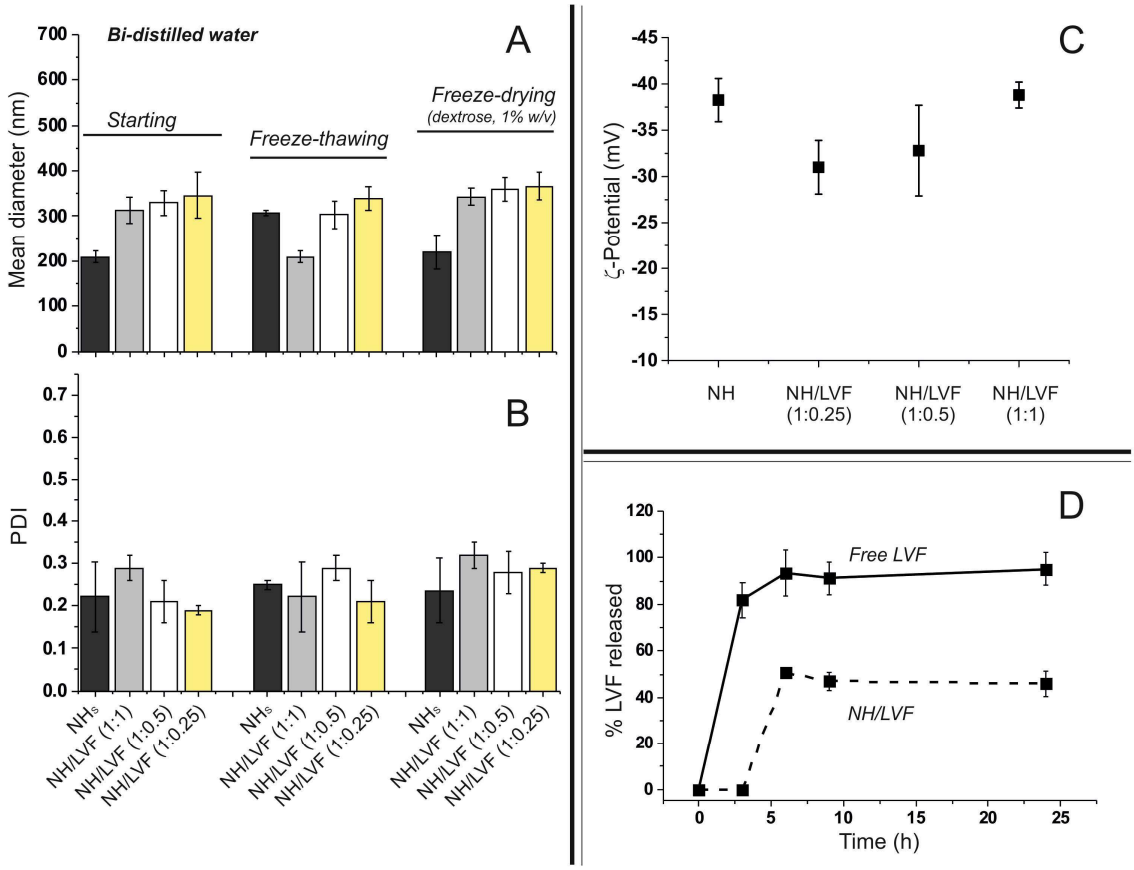

Figure 2. Mean diameter (A) and PDI (B) of starting, freeze-thawed and freeze-dried NH/LVF. HA-CH/LVF mixtures were prepared at several wt. ratios (ranging from 1:0.25 to 1:1 of HA-CH and LVF, respectively) in bi-distilled water and then autoclaved at 121°C for 20 min. Unloaded LVF was discarded by purification through a SEC column. (C) ζ-pot of NH/LVF samples and (D) release of LVF from NHs over 24 h at 37°C in bi-distilled water. LVF was detected with UV-Vis spectrometer. All data are expressed as the mean value ± standard deviation. Results were obtained in triplicate (n=3).

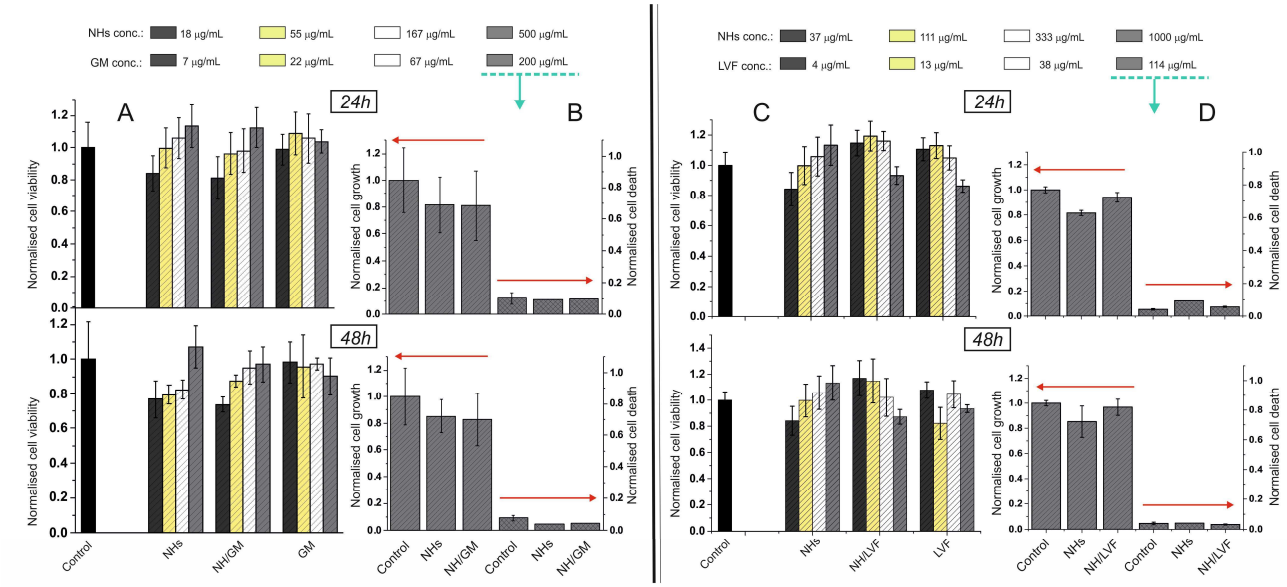

Figure 3. Viability of HaCaT: MTT (A and C) and trypan blue (B and D) assays were performed on cells cultured in completed DMEM, incubated for 24 and 48 h with NH/GM (A and B) and NH/LVF (C and D). Only samples with the starting 1:1 wt. ratio (HA-CH:drug) were tested. Results were obtained from three independent experiments (each derived from sixteen wells). All data are expressed as the mean value ± standard deviation. MTT and cell growth results were normalized to the control (untreated cells that received PBS), whilst the cell death was normalized to the total amount of cells. Statistical significance was determined with One-way ANOVA analysis. Differences between groups were determined by a Turkey's multiple comparison test. No significant differences were detected.

A

Sample	MIC (μg/mL)	MBC (μg/mL)
GM	15.6	15.6
NH/GM	15.6	15.6
LVF	11.7	15.6 ± 5
NH/LVF	11.7	15.6 ± 5
Free NHs	No activity	No activity

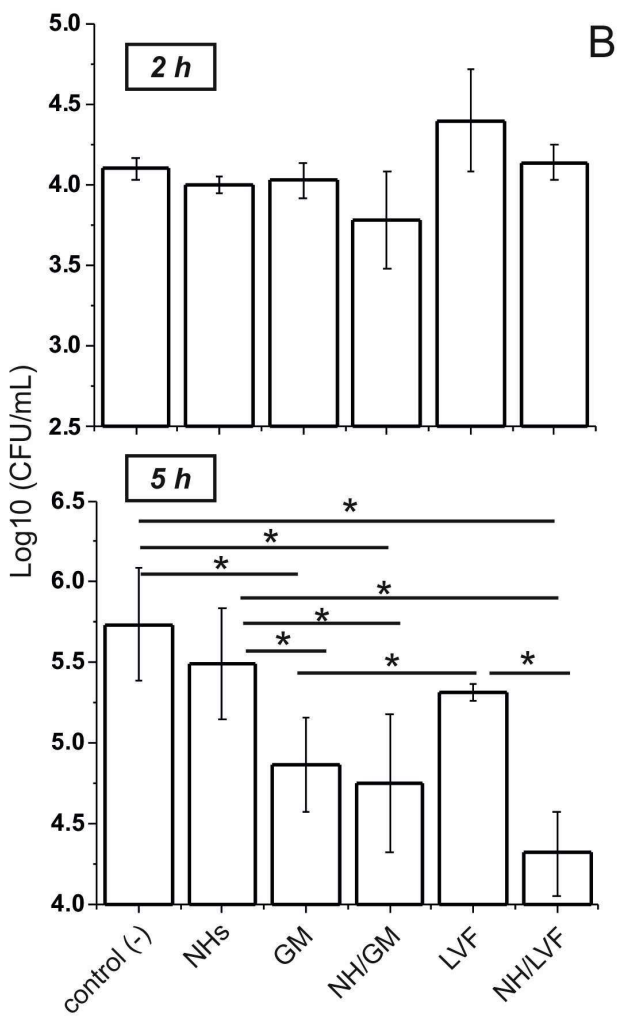

Figure 4. (A) MIC and MBC of NH/GM, NH/LVF and their controls against planktonic *S. aureus*. Plates were incubated for 24 h. The MIC endpoint was determined as the lowest concentration of antimicrobial at which there was no visible growth; the MBC endpoint was determined as the lowest concentration that resulted in no visual growth of colonies after 24 h of incubation. (B) Intracellular activity of NH/GM, NH/LVF and their controls against *S. aureus*-infected HaCaT. Viable cell counts were calculated using three biological replicate count data (each derived from three technical replicate data). All data were Log10 transformed and are expressed as the mean value ± standard deviation. Statistical significance was determined using biological replicate data (n=3) with Mann-Whitney test by using SPSS 20 Software. P values < 0.05 were considered significant. Asterisk denote statistically significant differences (*P<0.05).

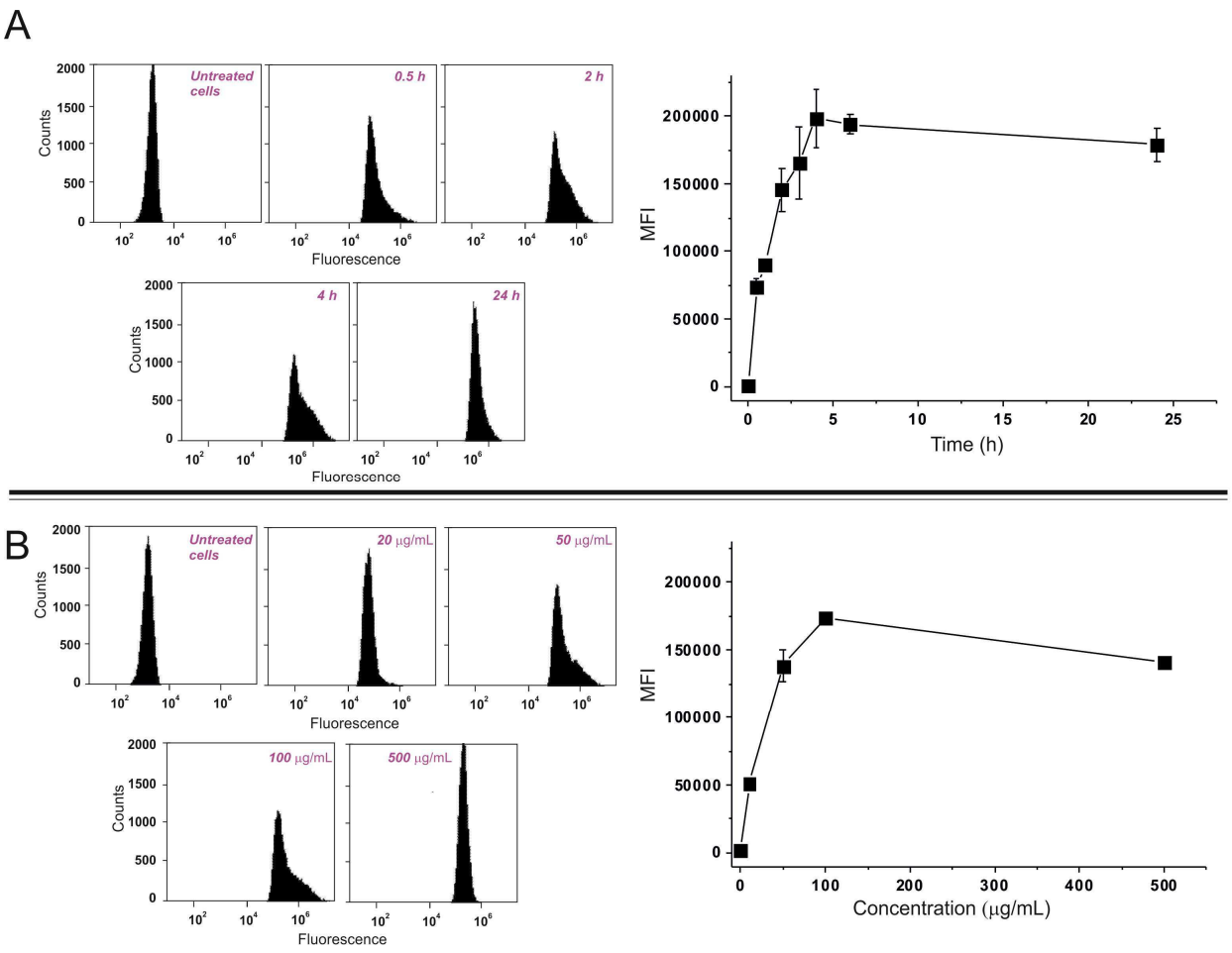

Figure 5. Flow cytometry analysis of HaCaT cells incubated with rhod-NHs. Cells were cultured in complete DMEM for 48 h and then incubated from 0.5 to 24 h with 100 μg mL^{-1} rhod-NHs (A) or with 20-500 μg mL^{-1} of rhod-NHs for 4 h (B). Results were obtained in triplicate (n=3). All data are expressed as the mean value ± standard deviation.

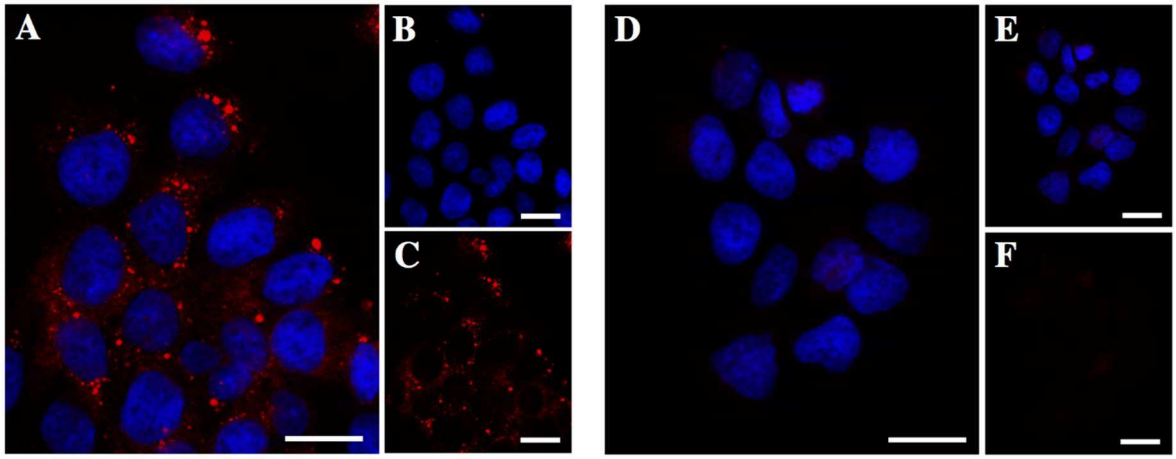

Figure 6. ApoTome micro-graphs (scale bars: 20 µm) of HaCaT cells incubated with 100 µg mL^{-1} rhod-NHs (A (merge), B (DAPI), C (rhod-NHs) or free rhod (D (merge), E (DAPI), F (rhod)). Cells were cultured in complete DMEM for 48 h and then incubated for 4 h with fluorescent nanoparticles.

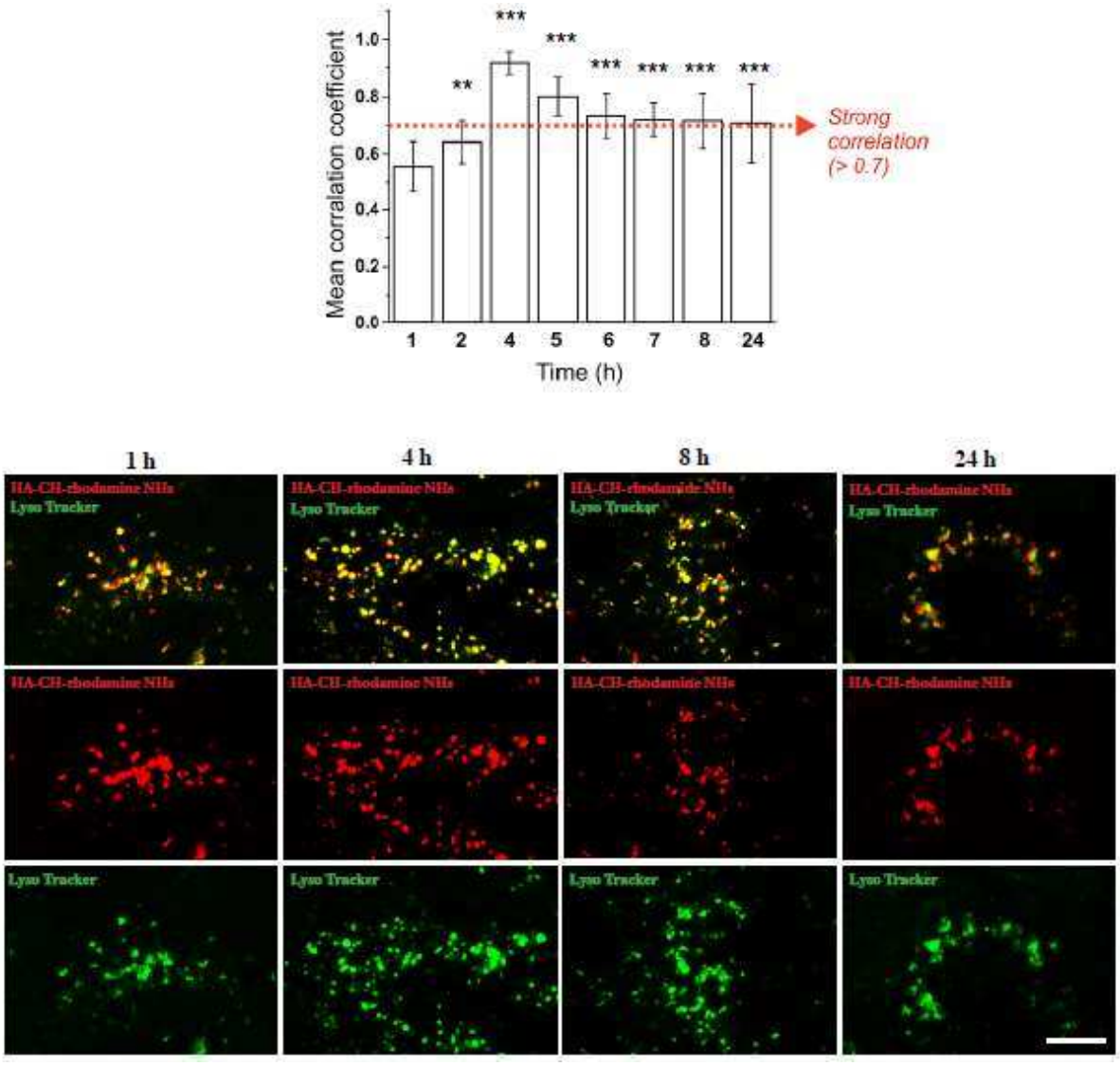

Figure 7. ApoTome micro-graphs (scale bar: 10 µm): co-localization with lysosomes. HaCaT cells were cultured in complete DMEM for 48 h and then incubated from 1 to 24 h with 100 µg mL^{-1} rhod-NHs. After specific time points slides were washed with PBS, added again to 1.5 mL of complete DMEM and finally treated with 1 mL of Lyso-Tracker Green' (final conc. of 200 nM) for 3 min at 37°C. Images were immediately recorded on living cells. Pearson's correlation coefficient was calculated using the AxioVision 4.8.2 software (Zeiss) and expressed as the mean value ± standard deviation. Results were obtained from three independent experiments, each derived from eight images. Statistical significance was determined with One-way ANOVA analysis. Differences between groups were determined by a Turkey's multiple comparison test. Asterisks denote statistically significant differences with the incubation time of 1 h (*P<0.05; **P<0.01; ***P<0.005).

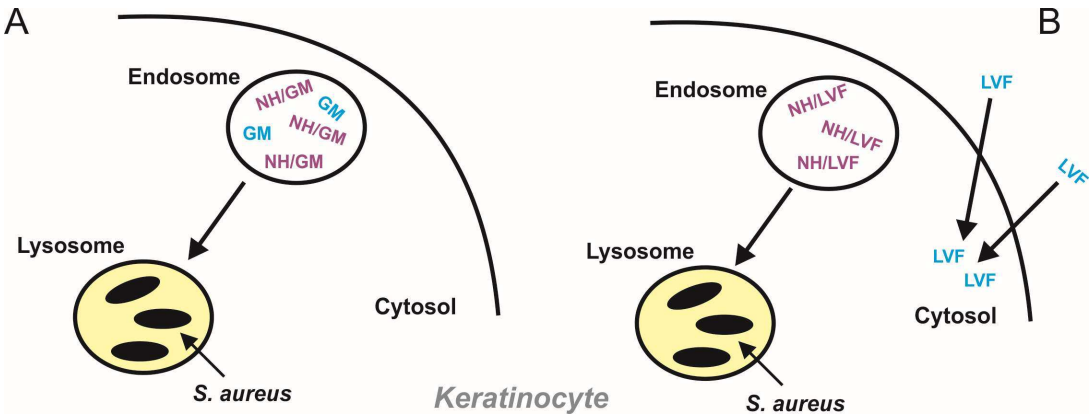

Figure 8. Scheme of the intracellular fate of free GM (A), LVF (B) and their nano-formulations in *S. aureus*-infected keratinocytes.

Table 1. Drug loading (DL, %) and loading efficiency (LE, %) of NH/GM and NH/LVF prepared at several HA-CH:GM or HA-CH:LVF wt. ratios (ranging from 1:1 to 1:0.25). Nano-systems highlighted (bold) were chosen for the biological and microbiological analyses. Experiments were performed in triplicate (n=3) and results are expressed as the mean value ± standard deviation.

Sample	DL%	LE%
NH/GM (1:1)	**40.0 ± 1.0**	**40.0 ± 1.0**
NH/GM (1:0.5)	35.1 ± 2.8	17.5 ± 1.4
NH/GM (1:0.25)	30.7 ± 2.0	7.7 ± 0.5
NH/LVF (1:1)	**11.4 ± 3.1**	**11.4 ± 3.1**
NH/GM (1:0.5)	9.5 ± 2.0	4.74 ± 1.0
NH/GM (1:0.25)	7.9 ± 0.8	2.0 ± 0.2